Design and Development of Microparticulate Delivery System of Metronidazole: Experimental Design Methodology

Raj Kumar Shukla,[1] Akanksha Tiwari[2]

[1]*School of Pharmaceutical Sciences, Rajiv Gandhi Proudyogiki Vishwavidyalaya, (Rajiv Gandhi Technological University), The State Technical University, Bhopal 462036, Madhya Pradesh, India*
[2]*Department of Pharmaceutics, Baroda College of Pharmacy, Parul Trust, Limbda, Waghodia-391760, Baroda, Gujrat, India*

Received 23 August 2011; accepted 24 January 2012
DOI 10.1002/app.36900
Published online in Wiley Online Library (wileyonlinelibrary.com).

ABSTRACT: This study describes the application of response surface methodology in the optimization of guar gum microspheres for colon-specific delivery of metronidazole. The effect of varying the relative percent of the four factors used, that is guar gum, glutaraldehyde, swelling time, and stirring speed, has been systematically investigated for identifying their best values to optimize the drug release and encapsulation efficiency as well as to highlight possible interactions among the components. Different batches were prepared according to 2^4 factorial designs and randomly evaluated for drug release and drug encapsulation efficiency. Analysis of response surface plots allowed identification of the best combination of four levels to minimize drug release in upper part of gastrointestinal tract and maximize the encapsulation efficiency. The scanning electron microscopy was used to characterize the surface of these microspheres. Drug polymer interactions were assessed by differential scanning calorimetry and XRD. The good correspondence between calculated and experimental values indicated in the validity of the generated statistical model. Only a small fraction of drug was released at acidic pH; however, the release of drug was found to be higher in the presence of rat cecal contents, indicating the susceptibility of crosslinked guar gum matrix to colonic enzymes released from rat cecal contents. Metronidazole release kinetics corresponds best to zero-order model and drug release mechanism was diffusion and swelling controlled. The significance of differences was evaluated by analysis of variance (ANOVA). Differences were considered statistically significant at $P < 0.05$. © 2012 Wiley Periodicals, Inc. J Appl Polym Sci 000: 000–000, 2012

Key words: colon delivery; response surface methodology; design of experiment; Guar gum; glutaraldehyde; crosslinking; metronidazole; microspheres

INTRODUCTION

Oral route is widely acceptable as it is convenient route of drug administration for the treatment of many local and systemic diseases but there is also disadvantage that most of the drugs are poorly absorbed through the gastrointestinal tract (GIT) membrane because some of the drug molecules are sensitive to the upper GIT environment, that is the presence of surfactants (bile salts), enzymes intracellular and extracellular sources and pH, thus it becomes challenges for the treatment of disease associated with the lower intestinal part, that is colon/large intestine. Hence, it is required to deliver the drug maximum drug load to the large intestine by reducing its degradation in upper GIT for the treatment of colonic diseases such as amebiasis, IBD, ulcerative colitis, colorectal cancer, and so on.[1–3]

Correspondence to: A. Tiwari (aksrgpv@gmail.com).

© 2012 Wiley Periodicals, Inc.

Amebiasis is a very common infection of the large intestine caused by *Entamoeba histolytica*, a single-celled protozoan parasite. Nitroimidazole derivatives are the drugs of choice used in the treatment of amebiasis, giardiasis, trichomoniasis, and anaerobic infections.[4,5] The drug is to be delivered to the colon for its effective action against *E. histolytica* where in the trophozoites resides in the lumen of the cecum and large intestine and adhere to the colonic mucus and epithelial layers.[6]

Various systems have been developed for colon-specific drug delivery they include enzymatically controlled system, coated with pH sensitive/biodegradable polymer, time dependent, osmotically controlled, and prodrug-based approach. Multiparticulate systems have several advantages over conventional single-unit systems such as more predictable rate of gastric emptying, site specificity, and fewer local adverse effects. The pH-sensitive polymers are not suitable for colon-targeted drug delivery systems because of the poor site specificity.[7,8]

Nowadays, naturally occurring polysaccharides such as guar gum (GG), chitosan, pectin, inulin, etc.,

TABLE I
Experiment Design—Levels of Process Parameters

Factors	Levels used			
	Low		High	
	Actual value	Coded value	Actual value	Coded value
X_1 = Polymer concentration; GG (% w/v)	1	−1	4	1
X_2 = Cross-linking agent; GL (% v/v)	0.5	−1	1.5	1
X_3 = Swelling time (h)	0	−1	4	1
X_4 = Stirring speed (rpm)	500	−1	1500	1
Response variable				
Y_1 = % Drug release				
Y_2 = % Encapsulation efficiency				

have attracted the attention to pharmaceutical scientists for colon-specific delivery. The carbohydrate polysaccharide GG is obtained from the seeds of *Cyamopsis tetragonolobus*. The structural units consist of linear chains of (1→4)-β-D-mannopyranosyl units with α-D-galactopyranosyl units attached by (1→6) linkages. There are 1.5–2 mannose residues for every galactose residue. GG hydrates rapidly in cold water to give highly viscous gel; this gelling property retards release of the drug in acidic environment of GIT and makes it susceptible to degrade in the colonic region.[9,10]

Design and formulation optimization of pharmaceutical dosage form presents high numbers of factors influencing the product development. Therefore, complex, expensive, and time-consuming studies are required for the development of products. The application of response surface methodology would provide an effective method to acquire the necessary information to understand the relationship among the factors and responses. Factorial designs are used in experiments where the effects of different factors or conditions, on experimental results, are the choice for simultaneous determination of the effect of several factors and their interactions. In factorial design, levels of factors are varied, each factor at two or more levels. The effects can be attributed to the factors and their interactions are assessed with the maximum efficiency in factorial design. Also, factorial design allows for the estimation of the effect of each factor and interaction unconfounded by other experimental study.[11]

The main objective of our research study was to design and develop crosslinked GG microspheres for colon-specific delivery of metronidazole (MZT) using response surface methodology.

MATERIALS AND METHODS

MZT (pure, 99.8%) was obtained from Dabur Pharma, India. Span-80 and GG (viscosity of 1% aqueous dispersion is 125 cps) was obtained from M/s Ranbaxy Lab., Gurgaon, India. Liquid paraffin and Glutaraldehyde (GL) were purchased from Merck, India. All materials used were of USP/NF quality.

Preparation of crosslinked GG microspheres of MZT (CMTZM)

Different batches of microspheres were prepared by water-in-oil (w/o) emulsification method. In brief, 20 mL aqueous dispersion of GG containing 20 % MTZ was acidified with 0.5 mL of dilute sulfuric acid solution and emulsified into 40 mL of liquid paraffin with 2% Span-80; GL was added in the solution to crosslink the GG. The mixture was stirred continuously using a mechanical stirrer for 4 h at room temperature. The hardened microspheres were filtered and washed repeatedly with hexane and water to remove unreacted GL, liquid paraffin, and any adhered Span-80. The microspheres were then dried at 40°C overnight and kept in desiccators until further use (Table I).

Experiment design

Systemic optimization procedure was carried out by selecting an objective function, finding the most contributing factors, and investigating the relationship between responses and factors. Objective function was selected as maximizing % encapsulation efficiency (EE) and minimizing % *in vitro* drug release (DR) in simulated gastrointestinal fluid (SGIF).

In this study, a two-level 2^4 factorial design was employed to evaluate the four independent factors and their influence on dependent factors.

A design matrix comprising 16 experimental runs was constructed using Design Expert 6.0 to investigate the effect of four factors, polymer concentration (X_1), crosslinking agent (X_2), swelling time (X_3), and stirring speed (X_4) on the response variable by Y_1 (% DR) and Y_2 (% EE). The various levels of experimental parameters are summarized in Table I.

The general model corresponds with the following equations:

TABLE II
2^4 Factorial Design and Effects of Process Parameters

Formulation	X_1 : % polymer concentration (w/v)	X_2 : crosslinking agent (mL)	X_3 : swelling time (h)	X_4 : stirring speed (rpm)	Y_1 : % drug release		Y_2 : % encapsulation efficiency		Particle size (μm)
					Actual	Predicted	Actual	Predicted	
1	1 (−1)	0.5 (−1)	0 (−1)	500 (−1)	21.30	21.26	60.44	60.88	30.24
2	4 (1)	0.5 (−1)	0 (−1)	500 (−1)	22.10	22.14	68.88	68.66	30.11
3	1 (−1)	1.5 (1)	0 (−1)	500 (−1)	25.20	25.24	64.35	65.14	28.76
4	4 (1)	1.5 (1)	0 (−1)	500 (−1)	24.48	24.44	66.43	65.86	28.44
5	1 (−1)	0.5 (−1)	4 (1)	500 (−1)	32.90	32.86	62.88	62.91	26.33
6	4 (1)	0.5 (−1)	4 (1)	500 (−1)	23.35	23.39	67.55	67.30	26.02
7	1 (−1)	1.5 (1)	4 (1)	500 (−1)	28.00	**28.04**	63.98	63.66	27.62
8	***4 (1)***	***1.5 (1)***	***4 (1)***	***500 (−1)***	***20.23***	***20.19***	***72.88***	***72.98***	***25.73***
9	1 (−1)	0.5 (−1)	0 (−1)	1500 (1)	24.20	24.24	62.88	62.44	23.12
10	4 (1)	0.5 (−1)	0 (−1)	1500 (1)	26.20	26.16	66.76	66.98	23.15
11	1 (−1)	1.5 (1)	0 (−1)	1500 (1)	32.00	31.96	64.86	64.07	20.03
12	4 (1)	1.5 (1)	0 (−1)	1500 (1)	27.80	27.84	67.44	68.01	22.22
13	1 (−1)	0.5 (−1)	4 (1)	1500 (1)	26.23	26.27	61.88	61.85	20.86
14	4 (1)	0.5 (−1)	4 (1)	1500 (1)	20.00	19.96	62.76	63.01	22.34
15	1 (−1)	1.5 (1)	4 (1)	1500 (1)	31.60	31.56	64.87	65.19	22.02
16	4 (1)	1.5 (1)	4 (1)	1500 (1)	31.20	31.24	77.86	77.76	22.37
CB1[a]	3	1.25	2.5	1200	26.18	27.28	67.54	68.72	25.41
CB2[a]	2.5	1.25	3	750	27.45	25.93	66.86	67.31	27.05
CB3[a]	2.0	1.0	2.0	1000	25.12	26.59	66.32	65.12	26.67
CB4[a]	1.50	1.0	2	1000	28.35	27.14	64.96	64.19	25.89

[a] The checkpoint batches prepared to validate the model.

$$Y = b_0 + b_1X_1 \ldots\ldots + b_4X_4 + b_{12}X_1X_2 + \ldots\ldots\ldots b_{123}X_1X_2X_3 + \ldots\ldots b_{1234}X_1X_2X_3X_4$$

where Y is the majored response associated with each factor level combination; b_0 is an intercept b_1–b_{234} are the regression coefficients; and X_1, X_2, X_3, and X_4 are the independent variables. The levels of selected variables are listed in Table I. These high and low levels were selected from the preliminary experimentation. The amounts of GG X_1, GL X_2, swelling time X_3, and stirring speed X_4, used to prepare each of the 16 formulations are listed in Table II.

Characterization of CMTZM

X-ray diffraction

The diffraction patterns were collected using a Bruker D8-Advance powder diffractometer, in θ–θ geometry, using CuK radiation and working at 50 kV and 40 mA. The Sol-X® solid-state detector was used. C/Ni Goebel mirrors in the incident beam were used as a monochromator; 1.0 mm divergence and scatter slits, and a 0.1 mm receiving slit were used.

Thermal analysis

Differential scanning calorimetry (DSC) thermograms were recorded with a DSC 2920 modulated Differential Scanning Calorimeter (TA Instruments, New Castle, DE). Samples weighing 5 mg (Precisa 262SMA-FR Balance) were heated in crimped aluminum pans from 30 to 300°C at a rate of 10°C min^{-1}. Nitrogen flow rate was 60 mL min^{-1}.

Size and surface morphology

Scanning electron microscopy (SEM) was used to characterize the surface and morphology of CMTZM and particle size was determined by using particle size analyzer (Cilas 1064 L, Marcoussis, France).

Encapsulation efficiency

EE was calculated in terms of the ratio of drug in the final formulation to the amount of drug initially loaded. An accurately weighed amount (100 mg) of the formulation of CMTZM was dispersed in 100 mL of phosphate buffer saline (PBS), pH 7.4. The sample was sonicated for 20 min. It was left to equilibrate for 24 h at room temperature and the suspension was then centrifuged at 1000 rpm for 20 min. The supernatant was diluted appropriately with PBS (pH 7.4) and analyzed for the concentration of MZT at absorbance wavelength $\lambda_{max} = 328$ nm using UV–visible spectrophotometer (UV-1700 CE by Shimadzu, Japan).

$$\%EE = \frac{(\text{spectorphotometrically determined amount of MTZ in final formulation})}{(\text{theoretically determined amount of MIZ in final formulation})} \times 100$$

(theoretically determined amount of MTZ in final formulation)

Swelling study

The equilibrium water uptake of the MTZ loaded and empty crosslinked GG microspheres were determined by measuring the extent of swelling in water. To ensure complete equilibrium, the samples were allowed to swell for 24 h. The excess liquid drops adhered on the surface were removed by blotting and the swollen microspheres were weighed. The microspheres were dried in oven at 60°C for 5 h, until there was no farther change in the dried mass of samples. The degree of swelling was then calculated from the following formula:

$$\text{Swelling index} = \frac{(\text{mass of swollen microspheres} - \text{mass of dry microspheres})}{\text{mass of dry micorsphers}} \times 100$$

DR study

In vitro DR study in simulated gastrointestinal fluid

SGIF: It consisted of simulated gastric fluid, pH 1.2, simulated intestinal fluid (SIF), pH 4.5 and 7.5.

The DR properties of the CMTZM were studied using a USP-II rotating paddle apparatus. The dissolution medium was maintained at 37 ± 0.1°C temperature and 100 rpm rotational speed and consisted of 900 mL of 0.1*N* HCl, pH 1.2, during the first 2 h of the dissolution test. After 2 h, the media pH was increased to 4.5 (SIF) by the addition of 0.2*M* NaOH. The dissolution media pH was increased to 7.5 after 3 h with the addition of a sodium hydroxide solution. A 5-mL sample was withdrawn every 1 h during the 8-h dissolution study and analyzed for MTZ using UV–visible spectrophotometer at absorbance wavelength λ_{max} = 318 nm. Sink conditions were maintained.

DR study in rat cecal contents

The study was carried out to check the ability of CMTZM to release the MTZ in presence of rat cecal content release medium resembling the physiological environment of colon.

Preparation of rat cecal content release medium

The medium was prepared by the method reported by Tiwari et al.,[7] Krishnaiah et al.,[12] and Van and Kinget.[13] The cecum bag was opened and its contents were weighed and homogenized, then suspended in phosphate buffer (pH 6.8) to give the desired concentrations (0, 2, and 4%) of cecal contents. The suspension was filtered through glass wool and sonicated (50 W) for 30 min at 4°C to disrupt the bacterial cells. After sonication, the mixture was centrifuged at 2000 rpm for 20 min. As the cecum's environment is naturally anaerobic, all the operations were performed in a CO_2 atmosphere, because it increases polysaccharidases activity.[14–16] The dissolution media used was 100 mL of pH 6.8 PBS containing (0, 2, and 4% w/v) of rat cecal contents (contained 150-mL beaker). The previously weighed amount of microspheres (an amount equivalent to 100 mg of MTZ) was placed in the dissolution media.

The samples (3 mL) were withdrawn after a fixed time interval, and the volume of dissolution media was replaced with fresh dissolution media. The studies were performed for 24 h; samples were diluted appropriately with PBS (pH 6.8) and centrifuged at 1000 rpm for 15 min. The supernatant was filtered through 0.45-μm Whatman filter paper and the filtrate was analyzed for MTZ content at λ_{max} = 325 nm using UV–visible spectrophotometer.

DR kinetics

To analyze the DR data, various kinetic models were used to describe the release kinetics. The zero-order rate, eq. (1), describes the systems where the DR rate is independent of its concentration.[17] The first order, eq. (2), describes the release from system where release rate is concentration dependent.[18] Higuchi[19] described the release of drugs from insoluble matrix as a square root of time-dependent process based on Fickian diffusion eq. (3). The Hixson–Crowell cube root law, eq. (4), describes the release from systems where there is a change in surface area and diameter of particles.[20]

$$C = k_0 t \tag{1}$$

where k_0 is zero-order rate constant expressed in units of concentration/time and t is the time.

$$\log C = \log C - kt/2.303 \tag{2}$$

where C_0 is the initial concentration of drug and k is first-order constant.

$$Q = Kt^{1/2} \tag{3}$$

where Q is the amount of drug dissolved in time t, K is the Higuchi dissolution constant.

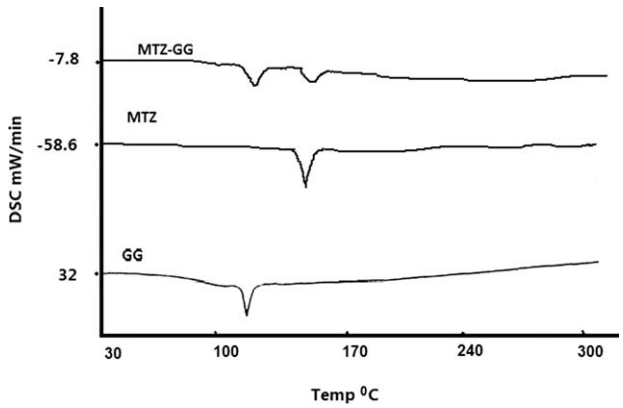

Figure 1 DSC thermograms of GG, MTZ, and crosslinked GG microspheres.

$$Q_0^{1/3} - Q_t^{1/3} = K_{HC}t \quad (4)$$

where Q_t is the concentration *of* drug released in time t, Q_0 is the initial concentration of the drug and K_{HC} is the Hixson–Crowell constant.

Mechanism of DR

Korsmeyer et al.[21] derived a simple relationship which described DR from a polymeric system eqs. (5) and (6). To find out the mechanism of DR, first 60% DR in data was fitted in Korsmeyer–Peppas model[21]:

$$M_t/M_\infty = Kt^n \quad (5)$$

$$\log\frac{M_t}{M_\infty} = \log K + n\log t \quad (6)$$

where M_t/M_∞ is fraction of drug released at time t, k is the rate constant and n is the release exponent. The n-value is used to characterize different release mechanisms. For spherical systems, when the value of n is $\leq$0.43 a Fickian diffusion-controlled release mechanism is applied. For n-value between 0.43 and 0.85, swelling controlled and diffusion controlled both controlled release mechanism is suggested. The value of $n > 0.85$ indicates the Case-II transport.[22,23]

RESULTS AND DISCUSSION

Thermal analysis

The DSC curve of MTZ and GG showed a single sharp peak at 165 and 111°C, whereas in the thermogram of CMTZM the intensity (or height) of the peaks was reduced, indicating an interaction of MTZ with GG (Fig. 1).

X-ray diffraction

X-ray diffraction patterns of MTZ, GG, and CMTZM are shown in Figure 4. X-ray diffraction of MTZ exhibited sharp diffraction peaks, indicating a crystalline nature. The diffraction peaks were much reduced in the case of the CMTZM. The disappearance of MTZ crystalline peaks could be attributed to dilution effect by the amorphous polymer [Fig. 2(a–c)].

Particle size and surface morphology

The particle size was determined by using particle size analyzer (Cilas 1064 L, Marcoussis, France). The average particle size was observed within range of 20–30 μm. Spherical-shaped and smooth surface particles were observed in electron microscope (Fig. 3).

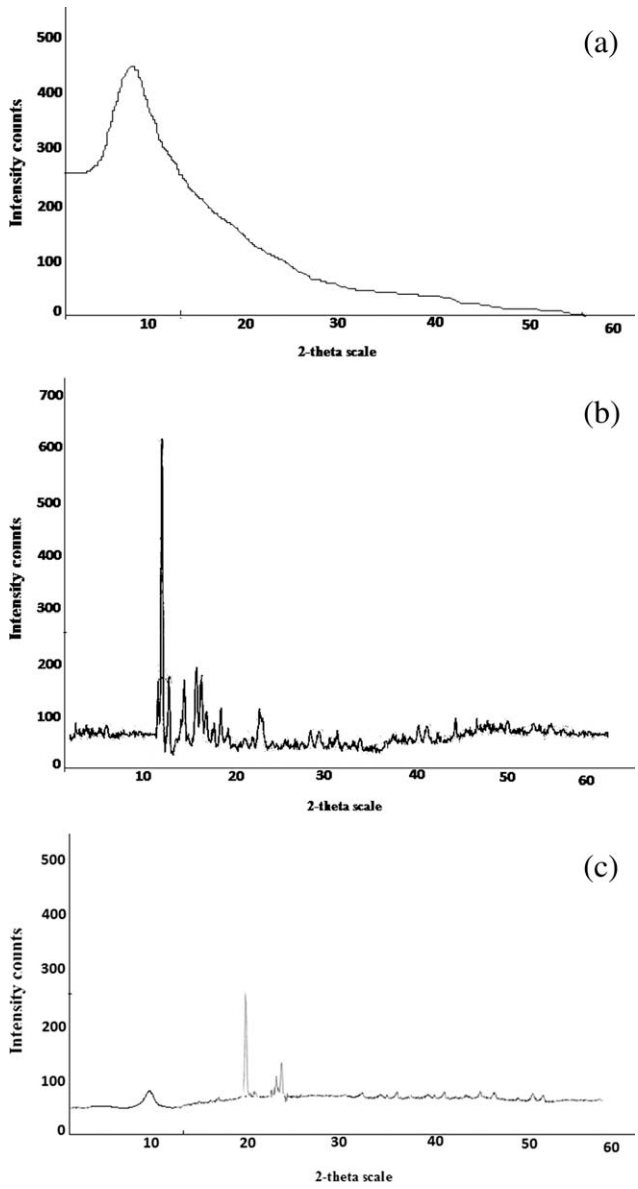

Figure 2 (a) XRD spectra of GG, (b) XRD spectra of MZT, (c) XRD spectra of crosslinked GG microspheres.

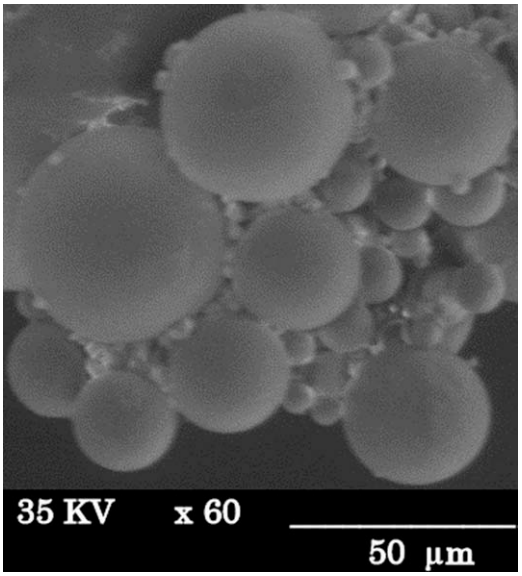

Figure 3 SEM of CMTZM.

Swelling index

The GG swells 100- to 150-fold in gastric and intestinal fluids. As a result of crosslinking with GL, the overall swelling of polymer decreased significantly. Crosslinking interferes with free access of water to the GG hydroxyl group, which in turn reduces the swelling properties of the crosslinked polymer. The crosslinking of the modified GG formulation depended on the GL concentration, but the optimal concentration of the crosslinking agent was a compromise between swellability and *in vitro* digestion of microsphere preparation in the presence of rat cecal content. The swelling index of CMTZM was found low (4.12–6.31) at acidic pH (1.2) but higher (27.89–38.06) at alkaline pH (7.4), indicating the ability of GG to resist the swelling at acidic pH (Table III). The swelling index is affected by gelling property of the polymer and diffusion rate at which water diffuses into the polymeric matrix. The swelling of GG allows more drug to be entrapped into the GG without increasing the polymer concentration. Consequently, a large amount of drug can be incorporated into the polymer and this leads to increase in EE, resulting in higher DR.

An increase in DR was observed with increase in swelling index and swelling time, owing to rapid hydration/high swelling, governed by dissolution, and diffusion of drug through the hydrated path in the polymer matrix formed by swelling. The release of water-soluble drug from the swellable matrix occurs only after the penetration of water into the polymeric matrix that allows swelling of the polymer and drug dissolution, following diffusion along the pathway to the surface of microspheres.[24,25]

Response surface methodology

To identify the key process, variables for experimental design, that influence the dissolution profiles and % EE of the GG microspheres independently, effect of the four parameters (polymer concentration, crosslinking agent, swelling time, and stirring speed) were studied by conducting the experimental runs at randomly selected different levels. Data were collected for DR from microspheres with respect to time in each run. These data were fitted into Design Expert® 6.0 and correlation coefficients along with other statistical parameters were estimated.

The mathematical relationship as polynomial equation for the measured response, % DR (Y_1) from CMTZM and % EE (Y_2) was as follows:

$$Y_1 = 26.05 - 1.63X_1 + 1.51X_2 + 0.64X_3 + 1.35X_4 - 6.875E - 003X_1X_2 + 0.53X_1X_4 - 0.45X_2X_3 + 1.7X_2X_4 - 0.79X_3X_4 + 0.96X_1X_2X_3 + 0.81X_1X_3X_4 + 1.34X_2X_3X_4 + 0.55X_1X_2X_3X_4.$$

$$Y_2 = 66.04 + 2.78X_1 + 1.79X_2 + 0.12X_4 + 1.27X_2X_3 - 0.11X_3X_4 + 1.50X_1X_2X_3.$$

A positive value represents an effect that favors the optimization, whereas a negative value indicates an antagonistic effect. The values of X_1, X_2, X_3, and X_4 were substituted in the equation to obtain the theoretical values of Y_1 and Y_2. The predicted value

TABLE III
Swelling Index Value of CMTZM at Different pH

	Swelling index at different pH			
	SGIF			PBS
Formulation	SGF (pH 1.2)	SIF (pH 4.5)	SIF (pH 7.4)	PBS (pH 6.8)
1	4.12	17.54	30.67	25.34
2	5.64	17.68	34.56	25.04
3	4.06	17.22	32.06	24.67
4	5.02	18.46	32.56	24.87
5	4.12	19.02	31.78	23.07
6	6.12	19.07	38.65	27.86
7	4.87	18.87	32.55	22.65
8	4.06	19.58	37.58	28.76
9	4.36	17.37	34.21	26.44
10	5.44	18.44	32.23	25.67
11	4.12	17.24	30.47	22.56
12	4.79	17.33	29.66	23.67
13	5.82	18.04	30.67	24.87
14	6.12	19.87	32.87	23.08
15	4.32	17.23	27.89	24.88
16	4.61	19.66	38.06	27.66
CB1[a]	5.68	18.95	34.08	22.87
CB2[a]	5.24	18.34	33.72	23.64
CB3[a]	4.85	17.04	30.23	25.88
CB4[a]	4.37	17.23	30.45	24.88

[a]The checkpoint batches prepared to validate the model.

TABLE IV
Individual and Combined Contribution of Independent Variables on Dependent Variables

Independent variables	Dependent variables					
	Contribution %		*F*-value		*P*-value Prob > *F*-value	
	Y_1	Y_2	Y_1	Y_2	Y_1	Y_2
X_1	15.78	42.71	1712.38	178.58	0.0154	0.0016
X_2	13.63	17.75	1479.20	74.24	0.0165	0.0002
X_3	2.43	3.44	263.68	14.41	0.0392	0.0010
X_4	10.90	0.080	1183.14	0.33	0.0185	0.0192
X_1X_2	2.810E−004	1.63	00.030	6.82	0.8900	0.5945
X_1X_3	11.07	2.37	1200.68	9.90	0.0184	0.0593
X_1X_4	1.64	0.31[a]	178.20	–	0.0476	–
X_2X_3	1.18	9.01	128.08	37.66	0.0561	0.0346
X_2X_4	17.83	3.58	1934.60	14.97	0.0145	0.0036
X_3X_4	3.67	0.067[a]	398.10	–	0.0319	–
$X_1X_2X_3$	5.46	12.46	592.11	52.13	0.0261	0.0180
$X_1X_2X_4$	9.218E−003[a]	3.62	[a]	15.15	–	0.0176
$X_1X_3X_4$	3.91	0.41[a]	423.84	–	0.0309	–
$X_2X_3X_4$	10.71	2.36	1161.40	9.90	0.0187	0.0346
$X_1X_2X_3X_4$	1.77	0.17[a]	192.02	–	0.0459	–

[a] These terms are not included in the model.

and observed value were found to be in good agreement (Table II).

Table IV summarizes the % contribution of each independent variable on dependent variable. Only those independent variables were included in the model that had a significant influence on dependent variables.

The % DR (Y_1) was observed significantly influenced by all factors. On the other hand, % EE was found to be more significantly influenced by polymer concentration (X_1), crosslinking agent (X_2), and swelling time (X_3) with % 42.71, % 17.75, and % 3.44 individual contributions, respectively (Table IV).

The correlation coefficients and other statistical parameters are listed in (Table V).

Figure 4(a,b) shows the observed and predicted % DR in and % EE, respectively. The observed values are in close agreement with predicted values, with $r^2 = 0.9736$ for % DR and $r^2 = 0.9787$ for % EE.

The effects of pairwise interaction of the parameters are depicted in the 2D and 3D graphs [Fig. 4(c–g)] when the other two parameters are kept constant.

The contour lines serve as a 2D representation of 3D surface. The contour plot [Fig. 4(c)] shows interaction between crosslinking agent and polymer concentration on % DR. The interaction was reflected by the lack of parallelism among the lines. When the polymer concentration was within the range of 3.4–4% and concentration of crosslinking agent was between 0.5 and 0.7%, the % *in vitro* DR showed minimum value (24%). Figure 4(d,e) portrays the 3D response surfaces. Figure 4(d) shows the combined effect of polymer concentration and crosslinking agent on % DR. Both the variables had antagonistic effect on % DR. Further increase in concentration of polymer decreased the DR. This may be owing to increase in thickness of polymer layer, and hence the diffusion distance of drug to diffuse out from the microspheres was increased. GL was crosslinked by reacting with the hydroxyl group of galactose and the mannose unit of the polymer GG, thus interfering with the free access of water to the hydroxyl group of GG. This significantly reduces the swelling of the microspheres and consequently the penetration of the water into the microspheres. Crosslinking also reduces polymer chain mobility, increases glass transition temperature, and decreases diffusivity.[24]

Figure 4(e) shows the combined effect of polymer concentration and swelling time on % DR. The swelling time had a positive effect on % DR. An increase in % DR was observed with increase in swelling

TABLE V
Statistical Parameters of Dependent Variables

Dependant variables	SD	Mean	C.V. (%)	r^2	Adjusted r^2	Predicted r^2	Adeq. precision
Y_1	0.16	26.05	0.60	0.9999	0.9986	0.9764	84.591
Y_2	0.83	66.04	1.26	0.9904	0.9641	0.8469	23.448

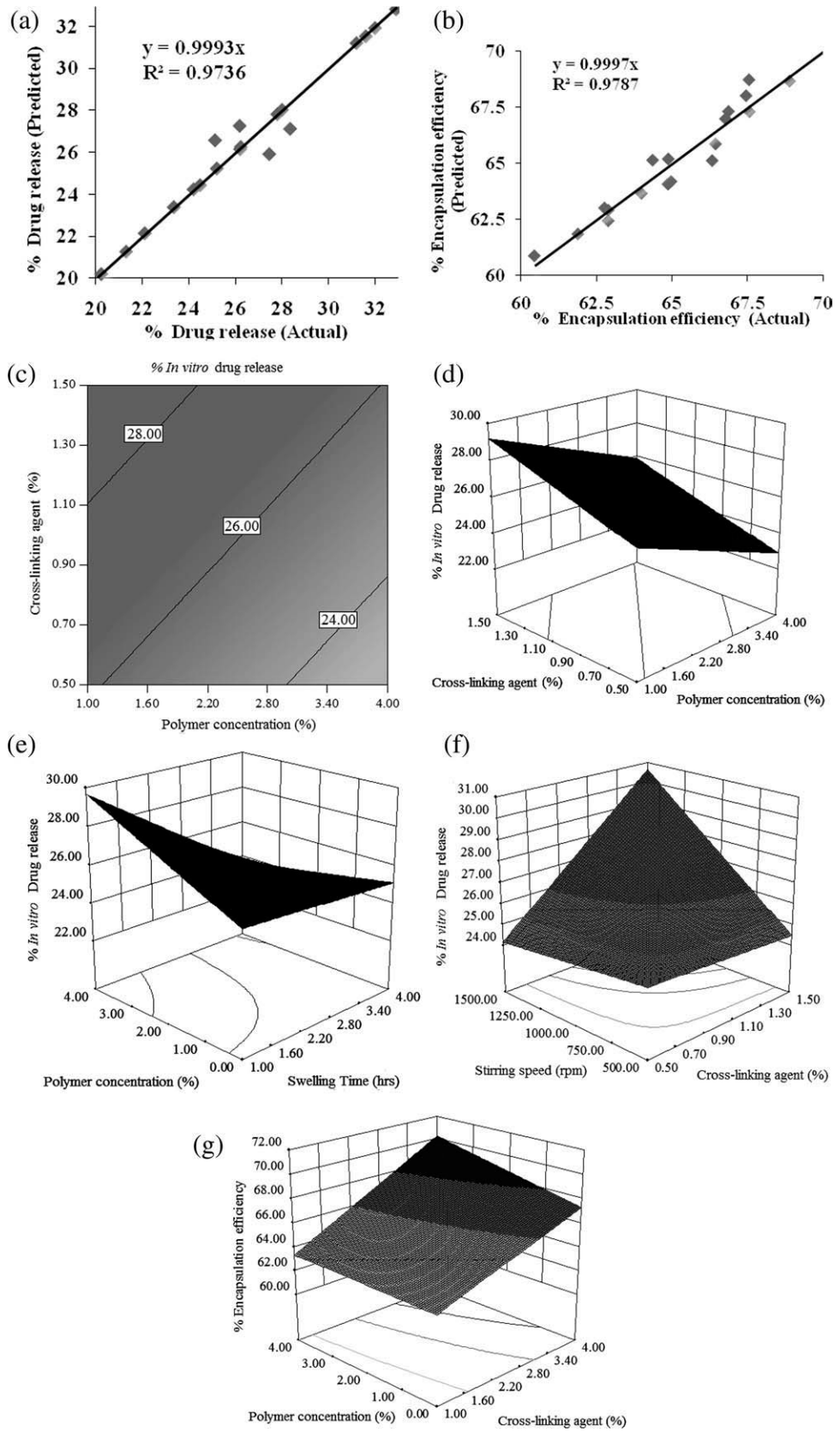

Figure 4 (a) % *In vitro* DR in SGIF (observed vs. predicted); (b) % EE (observed vs. predicted); (c) contour plot; effect of polymer concentration and crosslinking agent on % DR in SGIF; (d) combined effect of polymer concentration and crosslinking agent on % DR in SGIF; (e) combined effect of polymer concentration and swelling time on % DR in SGIF; (f) combined effect of stirring speed and crosslinking agent on % DR in SGIF; (g) combined effect of polymer concentration and crosslinking agent on % EE.

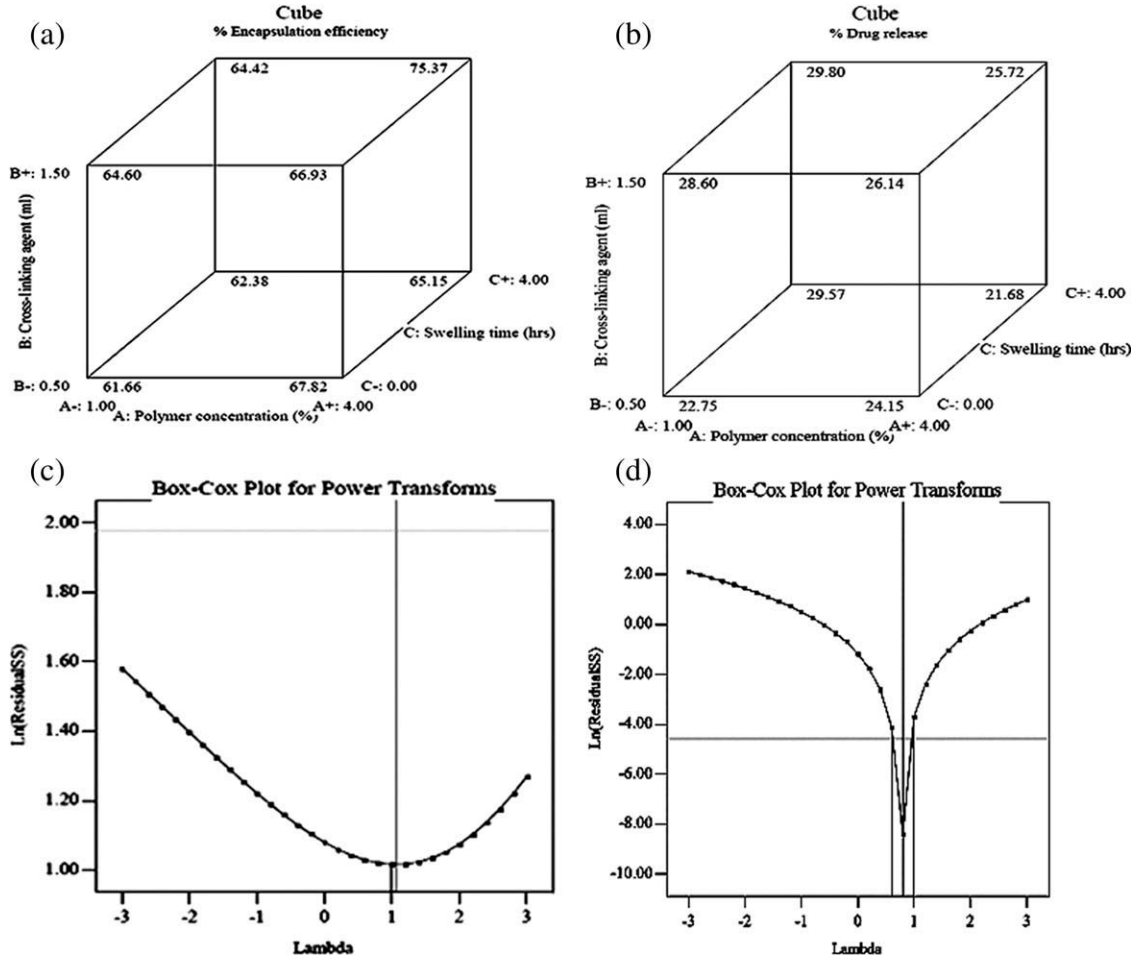

Figure 5 (a) Cube diagram—combined effect of crosslinking agent, polymer concentrations, and swelling time on % EE at constant stirring speed; 1000 rpm. $X_1 = A$; polymer concentration (%), $X_2 = \mathbf{B}$; cross-linking agent (mL), $X_3 = C$; Swelling time (h). *D*, stirring speed (rpm). (b) Cube diagram—combined effect of crosslinking agent, polymer concentrations, and swelling time on % DR at constant stirring speed; 1000 rpm. $X_1 = A$; Polymer concentration (%), $X_2 = B$; Crosslinking agent (mL). $X_3 = C$; Swelling time (h). *D*, stirring speed (rpm). (c) Box–Cox plot of % EE. Lamda Current = 1, Best = 1.07, Low C.I. = −5.15, High C.I. = 4.92. Recommended Transform, none. (d) Box–Cox plot of % DR. Lamda Current = 1, Best = 0.8, Low C.I. = 0.61, High C.I. = 0.98. Recommended Transform, Power ($\lambda = 0.8$).

time owing to rapid hydration/high swelling, governed by dissolution, and diffusion of drug through the hydrated path in the polymer matrix formed by swelling. The release of water-soluble drug from the swellable matrix occurs only after the penetration of water into the polymeric matrix that allows swelling of the polymer and drug dissolution, following diffusion along the pathway to the surface of microspheres.[25]

On the other hand, increase in polymer concentration initially increased the % DR up to maximum and then decreased. Figure 4(f) shows the combined effect of crosslinking agent and stirring speed on % DR, both variables had antagonistic effect. The 3D plot Figure 4(f) shows the synergistic effects of swelling time and polymer concentration on % EE, with the effect of polymer concentration being more pronounced. The swelling of guar gum allows more drug to incorporate into microspheres.

Figure 5(a,b) shows the cube diagram explaining the combined effect of crosslinking agent, polymer concentrations, and swelling time on % EE and % DR respectively, at constant stirring speed; 1000 rpm.

Figure 5(c,d) shows the Box–Cox plots for % EE and % DR, respectively.

The Box–Cox transformation is particularly a useful family of transformations. It is defined as:

$$T(Y) = (Y^{\lambda} - 1)/\lambda$$

where Y is the response variable and λ is the transformation parameter. For $\lambda = 0$, the natural log of the data is taken instead of using the above formula. Given a particular transformation such as the Box–Cox transformation defined above, it is helpful to define a measure of the normality of the resulting transformation. One measure is to compute the

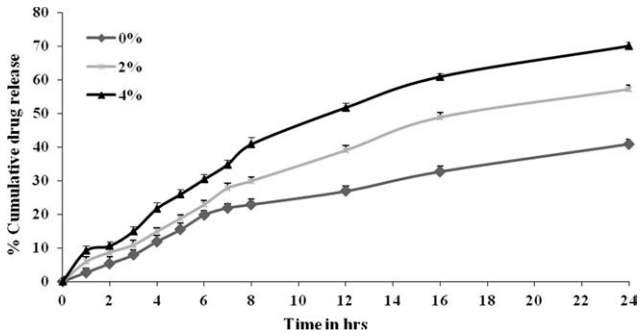

Figure 6 Mean (±SD) % cumulative DR in different concentrations of rat cecal contents (Formulation 8) ($n = 3$; $P \leq 0.05^{*}$, a); *Significant difference between 0 vs. 2% and 4%; a, significant difference between 2 and 5%.

correlation coefficient of a normal probability plot. The correlation is computed between the vertical and the horizontal axis variables of the probability plot and is a convenient measure of the linearity of the probability plot (the more linear the probability plot, the better a normal distribution fits the data). The Box–Cox normality plot is a plot of these correlation coefficients for various values of the λ parameter. The value of λ corresponding to the maximum correlation on the plot is then the optimal choice for λ.

Optimization of formulation

The optimum conditions for the preparation of crosslinked GG microspheres were selected on the criteria of attaining maximum entrapment efficiency and minimum DR in SGIF. The optimum conditions as evident from Table II, Figure 4, and Figure 5(a,b) are 4% (w/v) GG, GL 1.5 mL, swelling time 2 h, and stirring speed 500 rpm. The optimized Formulation 8 has the % DR in SGIF of 20.23 with 72.88% EE.

Validation of experimental model

The responses of the all formulations and four checkpoint batches were analyzed. The closeness of responses among actual and predicted values indicates the validity of developed experimental model (Table II).

Statistical analysis

Experimental data have been represented as the mean with standard deviation (SD) of different independent determinations. The significance of differences was evaluated by analysis of variance (ANOVA) using Design Expert® software, differences were considered statistically significant at $P < 0.05$.

DR in rat cecal content

In vitro DR in rat cecal content release medium was performed for the Formulation 8 (Table II) in different concentrations of rat cecal content. As the concentration of cecal content increased (0, 2, and 4%), the DR from the microspheres also increased. This could have been owing to the presence of bacterial polysaccharidases in rat cecal content which caused the degradation of GG.[7,26,27] Hence, it facilitated the release of drug from the microspheres. The maximum ~ 70% DR was observed (Fig. 6).

Kinetics and mechanism of DR

The DR kinetics of CMTZM correspond best to zero-order model ($r^2 = 0.9903$; Table VI) and DR mechanism as evident from Korsmeyer and Peppas (Power law) was diffusion and swelling controlled ($n = 0.81$).

An increase in MTZ release was observed with time owing to rapid hydration/high swelling, governed by dissolution and diffusion of drug through the hydrated path in the GG matrix formed by swelling. The release of water-soluble drug from the swellable matrix occurs only after the penetration of water into the polymeric matrix that allows swelling of the polymer and drug dissolution, following diffusion along the pathway to the surface of microspheres.[25]

When GG comes in contact with dissolution medium, it creates a viscous gel layer which controls the release of entrapped drug. The initial release of drug present was higher which could be owing to the fact that there was no viscous gel layer around microspheres and it might have formed after some times which controlled the further release of drug.[28]

The crosslinking of GG with GL inhibits the release of incorporated drug from the microspheres by suppressing the dissolution and swelling of GG microspheres. Nevertheless, it does not inhibit the diffusion of incorporated drugs from the surfaces of microspheres to the surrounding medium upon the drug's hydration. The release of drugs is affected by the mechanisms of drug diffusion and solvent activation.[29]

CONCLUSION

It was confirmed that experimental design methodology is a very useful tool in pharmaceutical preformulation studies, demonstrating that it is a very effective and rapid way to extract the maximum amount of information, and allowing to quickly

TABLE VI
Drug Release Kinetic Parameters of Different Models

Kinetic models	R^2	K (rate constant)
Zero order	0.9903	2.6460
First order	0.967	0.0278
Higuchi	0.8897	0.4586
Hixson–Crowell	0.9712	1.156
Korsmeyer and Peppas	0.9802	0.81

obtaining the best formulation. In fact % *in vitro* DR and the % EE of MTZ-loaded crosslinked GG microspheres have been optimized by using an experimental design methodology. The mathematical models generated by experimental design were valid and significant and allowed the identification of the best combination to obtain the highest drug EE and minimum DR in upper portion of GIT. The *in vitro* DR studies exhibited low DR at gastric pH; however, continuous release of drug was observed from the formulation at colonic pH. Further, the release of drug from formulation was found to be higher in the presence of rat cecal contents, explaining the effect of colonic enzymes on the MTZ microspheres. The most effective composition in this regard was GG % 4% (w/v), GL 1.5 mL, swelling time 4 h, and stirring speed 500 rpm. The closeness of calculated and experimentally determined values indicated the validity of the generated statistical models.

The authors are grateful to All India Institute of Medical Science (AIIMS), New Delhi–India for providing SEM facility.

References

1. Randall, J. M. J Control Release 1992, 22, 15.
2. Lee, V. H. L.; Mukkerjee, S. K. In Encyclopedia of Pharmaceutical Technology, 2nd ed.; Swarbrick, J., Boylan, J. C., Eds.; Marcel Dekker: New York, 2002: p 871.
3. Yang, L.; Chu, J. S.; Fix, J. A. Int J Pharm 2002, 235, 1.
4. Reynolds, J. E. F. Martindale—The Extra Pharmacopoeia; Pharmaceutical Press: London, 1996; p 380.
5. Weissman, S.; Salata, R. Nelson Textbook of Pediatric; W.B. Saunders Company: Philadelphia, 2000; p 1035.
6. Mc Coy, J. J.; Mann, B. J.; Petri, W. A. Infect Immun 1994, 62, 304.
7. Tiwari, A.; Ramteke, S.; Dahima, R.; Shukla, R. K. Curr Nano Sci 2011, 7, 608.
8. Ashford, M.; Fell, J.; Attwood, D.; Sharma, H.; Woodhead, P. Int J Pharm 1993, 95, 193.
9. Johnson, J. C.; Gee, J. M. Gut 1981, 22, 398.
10. Shukla, R. K.; Tiwari, A. Crit Rev Ther Drug Carrier Syst 2011, 28, 255.
11. Bolton, S.; Bon, C. In Pharmaceutical Statistics, Practical and Clinical Applications, 4th ed.; Marcel Dekker Inc.: New York, Basel, 2004; Vol. 135, p 506.
12. Krishnaiah, Y. S.; Veer Raju, P.; Dinesh Kumar, B.; Jayaram, B.; Rama, B.; Raju, V.; Bhaskar, P. Eur J Drug Metab Pharmacokinet 2003, 28, 287.
13. Vanden Mooter, G.; Kinget, R. Drug Deliv 1995, 2, 81.
14. Joel Dain, A.; Neal, A. L.; Seeley, H. W. J Bacteriol 1956, 72, 209.
15. Baileyr, W.; Oxforda, E. J Gen Microbiol 1958, 19, 130.
16. Ninomiya, K.; Matsuda, K.; Kawahata, T.; Kanaya, T.; Kohno, M.; Katakura, Y.; Asada, M.; Shioya, S. J Biosci Bioeng 2009, 107, 535.
17. Hadjiioannou, T. P.; Christian, G. D.; Koupparis, M. A.; Macheras, P. E. Quantitative Calculations in Pharmaceutical Practice and Research; VCH Publishers Inc.: New York, 1993; p 345.
18. Bourne, D. W. A. In Modern Pharmaceutics, 4th ed.; Banker G. S., Rhodes C. T., Eds.; Marcel Dekker Inc.: New York, 2002, p 67.
19. Higuchi, T. J Pharm Sci 1963, 52, 1145.
20. Hixson, A. W.; Crowell, J. H. Ind Eng Chem Res 1931, 23, 923.
21. Korsmeyer, R.W.; Gurny, R.; Doelker, E.; Buri, P.; Peppas, N. A. Int J Pharm 1983, 15, 25.
22. Siepmann, J.; Peppas, N. A. Adv Drug Delivery Rev 2001, 48, 137.
23. Pasparakis, G.; Bouropoulos, N. Int J Pharm 2006, 323, 34.
24. Deasy, P. B. Microencapsulation and Related Drug Processes; Marcel Dekker: New York, NY, 1984.
25. Singh, B.; Chauhan, N. Food Hydrocolloids 2009, 23, 928.
26. Salyers, A. A.; Palmer, J. K.; Wilkins, T. D. Am J Clin Nutr 1978, 31, 128.
27. Rubinstein, A. Biopharm Drug Dispos 1990, 11, 465.
28. Shukla, R. K.; Tiwari, A. Carbohydrate Polymers 2012, 88, 399.
29. Rubinstein, A.; Radai, R. Eur J Pharm Biopharm 1995, 41, 291.